

DOI: 10.1002/cbic.200800159

Nacre Calcification in the Freshwater Mussel *Unio pictorum*: Carbonic Anhydrase Activity and Purification of a 95 kDa Calcium-Binding Glycoprotein

Benjamin Marie,^{*,[a]} Gilles Luquet,^{*,[a]} Laurent Bédouet,^[b] Christian Milet,^[b] Nathalie Guichard,^[a] Davorin Medakovic,^[c] and Frédéric Marin^{*,[a]}

The formation of the molluscan shell is finely tuned by macromolecules of the shell organic matrix. Previous results have shown that the acid-soluble fraction of the nacre matrix of the freshwater paleoheterodont bivalve Unio pictorum shell displays a number of remarkable properties, such as calcium-binding activity, the presence of extensive glycosylations and the capacity to interfere at low concentration with in vitro calcium carbonate precipitation. Here we have found that the nacre-soluble matrix exhibits a carbonic anhydrase activity, an important function in calcification processes. This matrix is composed of three main proteinaceous discrete fractions. The one with the highest apparent molecular weight is a 95 kDa glycoprotein that is specific to

the nacreous layer. P95, as it is provisionally named, is enriched in Gly, Glx and Asx and exhibits an apparent pI value of ~4, or ~7 when chemically deglycosylated. Furthermore, its glycosyl moiety, consisting of sulfated polysaccharides, is involved in calcium binding. Purified fractions of the three main proteins were digested with trypsin, and the resulting peptides were analysed by mass spectrometry. Our results suggest that identical peptides are constitutive domains of the different proteins. Partial primary structures were obtained by de novo sequencing and compared with known sequences from other mollusc shell proteins. Our results are discussed from an evolutionary viewpoint.

Introduction

The molluscan shell is a classical biomineralisation product, composed of one or two polymorphs of calcium carbonate—calcite and aragonite—generally assembled in superimposed layers of different textures. One of them, the nacre or mother-of-pearl, is a fascinating example of a functional inorganic/organic composite, made of 95–99% aragonite and of 1–5% organic matrix.^[1–2] Nacre can be described as the compact juxtaposition of 0.5 μm -thick mineral tablets, surrounded by a thin organic layer.^[3] Although the organic matrix is quantitatively a minor component, it plays an important role for the elaboration of nacre.^[4] This matrix, a complex amalgamate of proteins, glycoproteins, lipids and polysaccharides including chitin, is secreted by the calcifying epithelium of the mantle, as are the mineral precursor ions.^[5] The matrix macromolecules are involved in critical functions such as the arrangement of a spatially ordered scaffold, the nucleation, the orientation and growth of calcium carbonate biominerals and the inhibition of their growth.^[6] Furthermore, the nacre matrix controls the calcium carbonate polymorph^[7] and exhibits cell-signalling properties.^[8] Finally, in one case it has been reported that the matrix exhibits a carbonic anhydrase activity,^[9] an important function for converting carbon dioxide into bicarbonate ions, one of the two reagents for the synthesis of calcium carbonate.

Numerous studies on mollusc shell have characterised the primary structures of proteins associated with nacre matrix (for recent reviews, see refs. [10], [11]). The nacre proteins often exhibit modular structures, composed of different functional domains.^[9,12–19] To date, about 15 complete sequences of effective

or putative proteins associated with nacre tissues have been described, but this number can be increased considerably if EST or proteomic approaches are used.^[20–23] In spite of the increasing amount of molecular data, it remains difficult to sketch the outline of the different protein families and domains involved in nacre formation, for a simple reason: all the data have been obtained from only four mollusc genera. It is unlikely that this sampling gives an accurate picture of the whole diversity of proteins associated with nacre.

On consideration of the huge size of the phylum Mollusca, and in view of the diversity of shell textures,^[24] one major question that arises involves the determination of the extent to which similar shell textures, present in different taxa, are produced by homologous sets of proteins. Bivalve nacre is particularly suitable for such an issue, because the nacreous texture is known in representatives belonging to four distinct subclasses: namely the Palaeotaxodonta, the Pteriomorphia, the

[a] Dr. B. Marie, Dr. G. Luquet, N. Guichard, Dr. F. Marin
UMR CNRS 5561 Biogéosciences, Université de Bourgogne
6, Bd. Gabriel, 21000 Dijon (France)
Fax: (+33) 3-80-39-63-87
E-mail: benjamin.marie@u-bourgogne.fr
gilles.luquet@u-bourgogne.fr
frederic.marin@u-bourgogne.fr

[b] Dr. L. Bédouet, Dr. C. Milet
UMR CNRS 5178, Biologie des Organismes Marins et Ecosystèmes
MNHN, 75231 Paris (France)

[c] Dr. D. Medakovic
Center for Marine Research Rovinj
52210 Rovinj (Croatia)

Palaeoheterodonta and the Anomalodesmata.^[25–26] However, all the available molecular data have been retrieved only from the Pteriomorphia (*Pinctada* and *Pinna* genera), and no data for the three other subclasses have been published so far. This paper consequently represents a first step in characterizing the proteins associated with nacre in one Palaeoheterodont bivalve, in order to compare the nacre proteins of both groups. To this end we selected the freshwater unionoid bivalve *Unio pictorum*, which has an entirely aragonitic nacre-prismatic shell. In a recent paper we characterised the whole organic acid-soluble matrix (ASM) of the nacreous layer of *U. pictorum*.^[27] In this paper we use the combination of biochemistry and proteomics for further characterisation of the shell matrix. In particular, we report the presence of a noteworthy carbonic anhydrase activity within the ASM matrix and we biochemically characterise P95, a nacre-specific glycoprotein capable of binding calcium ions. Finally, we have obtained a set of partial sequences of nacre mollusc shell proteins by mass spectrometry.

Results

Shell matrix characterisation on gels

Figures 1 A and B show the two microstructures that make up the shell layers of *U. pictorum*—the nacre (Figure 1 A) and the outer prisms (Figure 1 B), respectively—and from which their corresponding ASMs were extracted. Figure 1 C shows the electrophoretic patterns of the two ASMs, stained with Coomassie

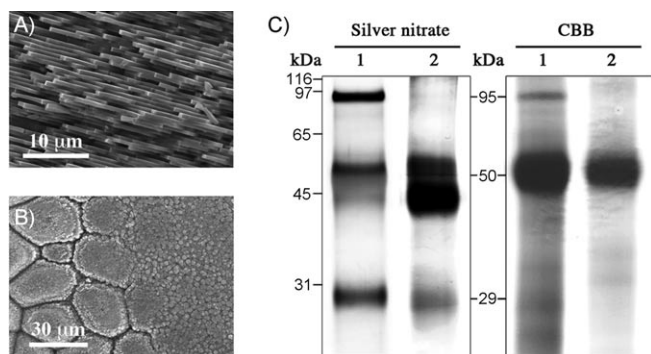


Figure 1. The shell of *U. pictorum* and associated skeletal matrices. A) SEM micrograph of a cross-section of the nacreous layer. B) SEM micrograph of the transition zone between the prisms (on the left, outer shell layer) and nacre tablets (on the right, internal shell layer), observed on the internal shell surface. C) Electrophoresis analysis of the acid-soluble matrices (ASMs) of the nacreous and the prismatic layers (wells 1 and 2, respectively) on 12% SDS-PAGE stained with silver nitrate and CBB.

brilliant blue (CBB, right) and with silver nitrate (left). The two extracts are characterised by a few prominent discrete bands, in addition to a smear, particularly visible on CBB staining. Two bands, at about 50 and 29 kDa, are present in the two matrices. On the other hand, a protein migrating at 95 kDa, provisionally called P95, is observed exclusively in the nacreous layer, whatever the staining procedure used. We noticed that the electrophoretic pattern depends on the freshness of the

shells; the intensity of the P95 band tends to decrease, for example, in extracts from “old” shells (collected years after the death of the animal), which also have a different appearance (not shown).

Carbonic anhydrase activity of the nacre ASM

Since a carbonic anhydrase (CA) activity had previously been detected in the nacre of one pteriomorphid bivalve (*Pinctada* sp.), we investigated the CA activity in the nacre ASM of *U. pictorum*, by using Maren’s phenol red colorimetric test.^[28] The histogram in Figure 2 shows that the ASM extract exhibits

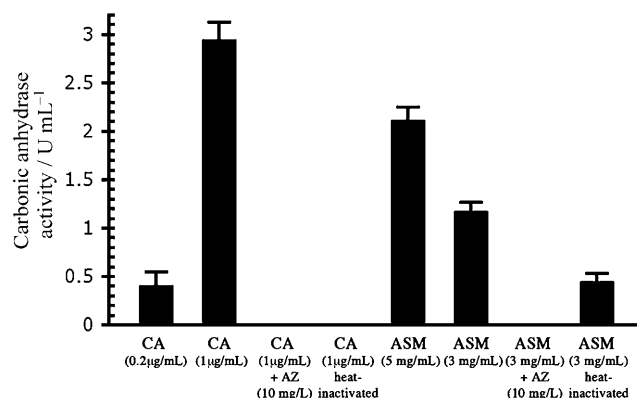


Figure 2. Carbonic anhydrase activity of the nacre ASM of *U. pictorum*. Commercial carbonic anhydrase (CA) from bovine erythrocytes was used as a positive control, and acetazolamide (AZ) was used as specific inhibitor of carbonic anhydrase activity. Each value is the average of three measurements.

a notable CA activity, as in the case of the bovine erythrocyte CA control. The ASM extract indeed exhibits an activity of 2.1 units mL⁻¹ of CA for a 5 mg mL⁻¹ concentration and of 1.2 units mL⁻¹ for a 3 mg mL⁻¹ concentration. This corresponds to a mean specific activity of 0.4 units per mg of matrix. The activities both of the control and of the ASM are dose-dependent. Furthermore, they are sensitive to acetazolamide inhibitor and to heat denaturation, which in the nacre of *U. pictorum* corresponds to true enzymatic activity. In the case of the heat denaturation of the ASM, however, we noticed that a residual activity, representing one third of the activity of the untreated extract at the same concentration, could still be seen after 10 min at 100 °C. One explanation might be that some enzymatic sites may remain sterically protected even after heat treatment.

P95 characterisation

P95 was found to be specific to the nacreous layer. It was consequently investigated further. Fractionation of the nacre ASM by preparative electrophoresis resulted in the effective one-step purification of P95. The purity of the P95 extract was checked by 1D gel electrophoresis with silver nitrate staining (Figure 3 A, lane 2). A polyclonal antibody raised against puri-

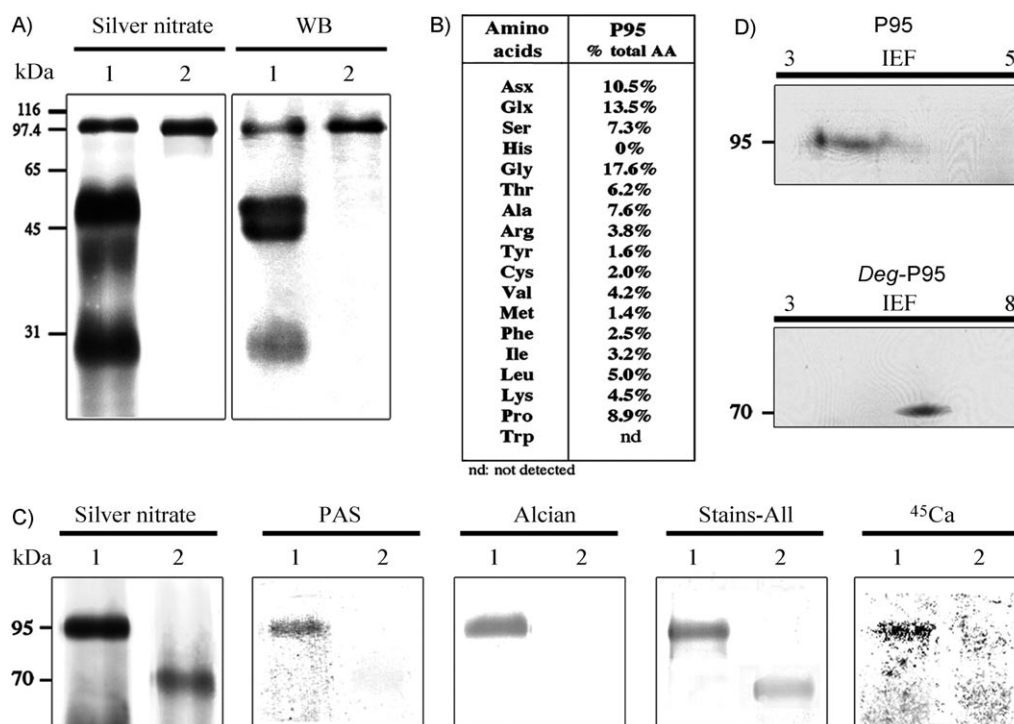


Figure 3. Purification and characterisation of P95, a nacre-specific ASM protein. A) 12% SDS-PAGE of the nacre ASM (lane 1) and of the purified P95 (lane 2), stained with silver nitrate. The same extracts were tested on Western blot incubated with the anti-P95 polyclonal antibodies. Note that the antibodies cross-react with the other discrete components of the ASM. B) Amino acid composition of the purified P95. Asx = Asn + Asp; Glx = Gln + Glu; tryptophan residues are destroyed during the hydrolysis. C) Two-dimensional gels of purified P95 and TFMS-deglycosylated P95 (*deg*-P95), stained with CBB. D) 10% minigels of P95 (lane 1) and *deg*-P95 (lane 2), stained with silver nitrate, PAS, Alcian blue and Stains-All, and PVDF membrane revealed by autoradiography with ⁴⁵Ca.

fied P95 was tested against P95 and against the ASM. The results, shown besides the silver nitrate staining (Figure 3A) indicate a strong cross-reactivity of the antibody preparation with all the discrete components of the ASM. The antibody staining is slightly more discriminatory than the silver nitrate: the thick band at 50 kDa is indeed not homogeneous, but dissociates into two bands of close apparent molecular weight. The cross-reactivity of the antibodies may be explained by P95 and the other discrete components having oligosaccharidic or protein epitopes in common.

The extract was analysed further for amino acid composition. Figure 3B shows that the four dominant amino acid residues are Gly (17.6%), Glx (13.5%), Asx (10.5%) and Pro (8.9%). In comparison with the amino acid composition of the bulk matrix,^[27] P95 is enriched in Glx and Pro residues, but depleted in Ala and Asx residues. The sum of aliphatic residues is above 37%. The high level of aliphatic residues, on one hand, and of the sum of aspartate and glutamate residues, on the other, is the signature of several molluscan shell proteins. Interestingly, a search based on similarity of amino acid composition (AA-Complident, <http://expasy.org/tools/aacomp/>) identified several C-type lectins. From previous works, it is known that C-type lectins may be constituents of calcifying matrices.^[13,14]

Periodic acid–Schiff (PAS) and Alcian blue staining on SDS-PAGE suggest that P95 is an acidic glycoprotein (Figure 3C). In addition, Stains-All staining of P95 in blue and ⁴⁵Ca overlay test both demonstrate that P95 binds calcium ions. To characterise its glycosyl moieties further, P95 was chemically deglycosylated

with trifluoromethanesulfonic acid (TFMS) at 0 °C, and the resulting extract was called *deg*-P95. When run on a gel, *deg*-P95 shows a significant shift of about 25 kDa (from 95 to 70 kDa of apparent molecular weight). This shift is primarily the result of the loss of covalently bound polysaccharides. It may also, secondarily, be the result of a difference in the amount of negative charges (due to SDS) surrounding the denatured P95 and *deg*-P95. The removal of linked polysaccharides is characterised by a drastic reduction in the PAS staining and by the complete disappearance of the Alcian blue staining. Because we had used Alcian blue under low pH conditions, this clearly suggests that the sugar moieties of P95 are sulfated. Furthermore, *deg*-P95 stains red with Stains-All and does not bind calcium ions in the ⁴⁵Ca overlay test. This clearly demonstrates that the calcium-binding ability of P95 is a property of its glycosyl moieties.

The 2D gel shows that the P95 band is acidic with at least six or seven isoforms clustered around pI values ranging from 3.5 to 4.3 (Figure 3D, top). After the chemical deglycosylation, *deg*-P95 is focussed as a single spot at a pI value between 6.5 and 7 (Figure 3D, bottom). This suggests that the P95 extract is a single protein, which exhibits different glycosylation patterns, carrying different negative charges. Calculation of the theoretical pI of the protein core (http://www.expasy.ch/tools/pi_tool.html) from its amino acid composition indicates a pI between 4 and 10, depending on whether the Asx and Glx residues are in their acidic or amine forms. Since *deg*-P95 has a neutral pI, our computer simulation estimates that half of the Asx + Glx residues of P95 are in their acidic forms.

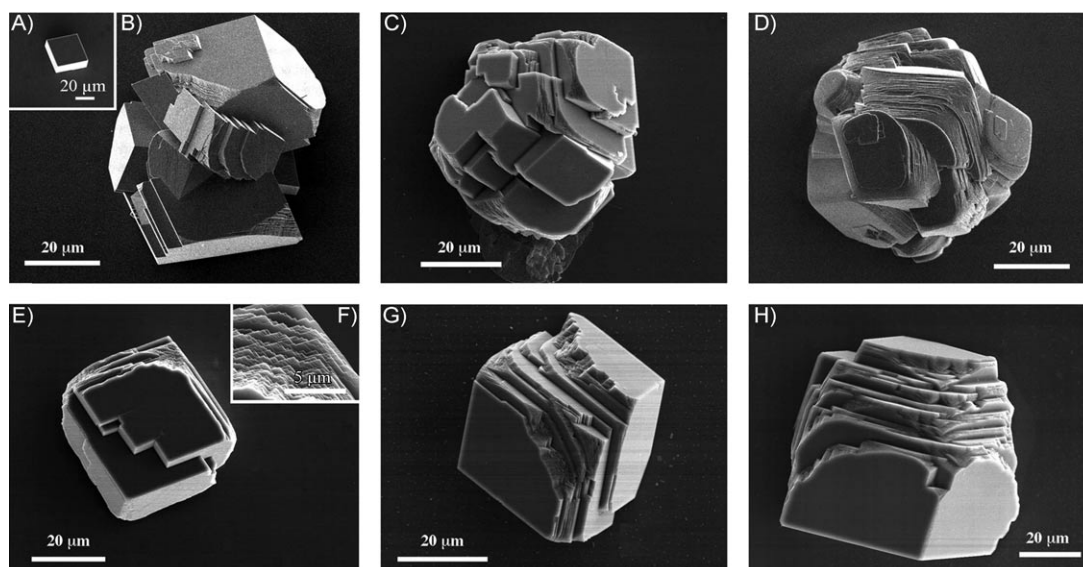


Figure 4. SEM micrographs of synthetic calcium carbonate crystals grown in vitro: B–D) with nacre ASM, and E–H) with purified P95, at concentrations ranging from 0.1 to 10 $\mu\text{g mL}^{-1}$. A) Negative control. B) ASM (0.5 $\mu\text{g mL}^{-1}$). C) ASM (2 $\mu\text{g mL}^{-1}$). D) ASM (10 $\mu\text{g mL}^{-1}$). E) P95 (0.5 $\mu\text{g mL}^{-1}$). F) Detail of (E). G) P95 (2 $\mu\text{g mL}^{-1}$). H) P95 (10 $\mu\text{g mL}^{-1}$).

CaCO₃ precipitation interaction test

The CaCO₃ precipitation interaction test is commonly performed with macromolecules associated with calcitic or aragonitic structures to investigate their effect in calcium carbonate precipitation.^[18,29–31] To estimate the effects of P95 on the morphology of calcium carbonate crystals, we examined crystals obtained in the presence of P95 by SEM and compared the results with those of a positive control experiment performed with the whole nacre ASM (Figure 4). Negative control experiments produced the typical calcite rhombohedrons (Figure 4A). In the presence of increasing amount of nacre ASM (0.5–10 $\mu\text{g mL}^{-1}$; Figure 4B–D), the produced precipitates appear mostly as polycrystalline aggregates (60–80 μm diameter). At 10 $\mu\text{g mL}^{-1}$ ASM, crystals exhibit foliation with microsteps and rounded corners (Figure 4D). At the highest concentration (20 $\mu\text{g mL}^{-1}$ ASM), the precipitation of calcium carbonate starts to be inhibited, which results in the production of small-sized crystals (not shown). Similar effects were found with shell nacre matrices.^[31]

In the presence of P95, we do not observe any polycrystalline aggregates. Furthermore, the overall morphology of monocrystals grown in the presence of P95 develops with numerous supernumerary faces organised in microsteps (Figure 4E–H). Even at the highest concentrations of P95 (up to 20 $\mu\text{g mL}^{-1}$), no inhibition of precipitation occurs. We note that the effect on crystal morphology is smaller with P95 alone than with the complete ASM; this suggests a synergistic effect of the different ASM components in interacting with the precipitation of carbonate crystal, as proposed by Matsushiro et al.^[32]

Proteomics analysis

In a first approach, we investigated the primary structure of *U. pictorum* shell proteins by N-terminal sequencing of purified proteins with preparative electrophoresis, but unfortunately no peptidic sequence was obtained, as the proteins appeared to be a mixture of isoforms of the same masses or were N-terminally blocked. Subsequently, we performed two-dimensional electrophoresis (2DE) separation followed by internal sequencing. Two-dimensional electrophoresis of nacre ASM gave satisfactory resolution for the separation of proteins,^[27] and five main spots were unambiguously excised from the gel for de novo sequencing (Figure 5). All the protein spots digested with trypsin were firstly analysed by MALDI-TOF/TOF in MS and MS/MS modes. No hit was found by peptide mass fingerprint (PMF) search with the MASCOT tool of the ExPASy server, indicating that the obtained peptides do not correspond to already known sequences from the databases. Because of the

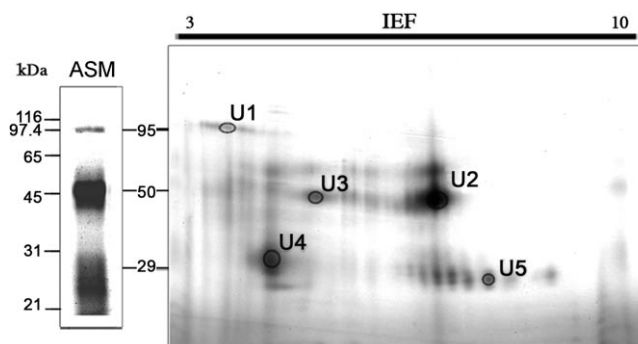


Figure 5. Proteomic analysis of *U. pictorum* nacre proteins. A) Separation of nacre ASM by 2D electrophoresis and coloration with CBB. Spots analysed by MS after trypsin digestion were named U1–U5.

absence of genomic data on freshwater mussels and in view of the diversity of the already sequenced mollusc shell proteins, it is not surprising that PMF searching cannot provide a reliable result for identifying proteins. On the other hand, the m/z values of these peptides indicate that the different spot proteins share numerous peptides of the same m/z , especially the spots U2 and U5 (Table 1), suggesting that different proteins of the nacre ASM may share similar peptide sequences. This was confirmed by analysis of the most abundant peptides in the MS/MS mode for de novo sequencing: peptides of the same m/z , such as 1313.7 from spots U2 and U5, share the same spectrum pattern. This indicates that some of the protein spots analysed on MS have amino acid sequences in common. It is important to note that, in spite of these similarities, the U2 and U5 digest patterns exhibit several non-common peptides (Table 1). This precludes the possibility of contamination between these two spots. We can also exclude the possibility that P95 and/or P50 are the results of polymerisation of P29 monomers, because they exhibit very different charges. However, this does not rule out the eventuality that the higher molecular weight proteins may be preferentially cleaved into smaller fragments: P29 (spot U5), for example, could be a cleavage product of P50 (spot U2).

As the digestion of the U1 spot (corresponding to P95) gave very few peptides, due to the insufficient amount of protein material present in a spot, purified P95 was also similarly analysed. We observed that the intensive digestion of P95 with trypsin yielded 28 to 33 peptides (Table 1), which is less than expected (about 70) from the size of deglycosylated P95 and its basic amino acid residue (Arg + Lys) composition. This suggests that some cleavage sites may be masked by the glycosyl moieties of P95.

Sequence analysis and homology search

Partial sequences of the ASM nacre proteins were obtained by interpretation of a MS/MS spectrum for de novo sequencing (Figure 6). The analysis of mass differences between ions was assisted by the Rapid De Novo software and all obtained sequences were further manually confirmed. We only consider amino acid positions that were definitely determined. Uncertain amino acids are mentioned in brackets. We obtained full or partial peptide sequences only for the U2 and U5 spots or the P95 purified proteins by MALDI-TOF/TOF analysis (Table 2). Few peptides analysed in MS/MS mode could be fractionated or gave good MS/MS spectra for amino acid sequence interpretations. It is likely that some of the trypsin digests bear glycosyl moieties or other post-translational modifications, which restrain the MS/MS fractionation and spectra interpretation.

A homology search was performed with the WU-BLASTP program against the Swiss-Prot protein nonredundant database, but no relevant similarity was obtained. A complementary SIM analysis was performed with each obtained sequence aligned two-by-two with those of the known molluscan shell proteins.^[11] We observed that the newly obtained sequences of *Unio* nacre ASM do not exhibit homology with other mollusc shell proteins, except for the Gly-repeat of the 1457.57 m/z peptide of the P95, which partly matches (five aa residues) with several short motifs of the acidic proteins: MSI31 [O02401], MSI60 [O02402] and MSI7 [Q7YWA5]. These similarities may be fortuitous, and may or may not have any phylogenetic implications.

Discussion

One of the challenges for understanding molluscan shell biomineralisation is the thorough biochemical and functional characterisation of the matrix macromolecules associated with

Table 1. m/z values of the main peptides from excised 2DE spots U1–U5 (see Figure 5) or from the purified P95 (Figure 3A, lane 2) after digestion with trypsin. The data were obtained by MALDI-TOF/TOF.

Protein name	m/z values (singly charged ions)
P95/spot U1	<u>2029.98</u> , 2057.00, <u>2069.99</u> , 2084.04, 2812.02
P50/spot U2	1002.35, 1003.37, 1073.45, 1086.47, 1097.26, 1113.44, 1127.45, <u>1130.48*</u> , 1162.47, 1256.64, 1269.65, <u>1286.32</u> , <u>1313.68*</u> , 1329.66, 1335.64, 1345.67*, 1351.64*, <u>1363.69*</u> , <u>1379.69*</u> , 1408.91, <u>1531.56</u> , 1550.65*, 1603.70, <u>1647.71*</u> , 1685.66, 1694.03, 1701.57, 1704.72*, 1718.75, 1724.57, 1748.81*, 1759.83, 1761.81*, 1787.79, 1804.84*, <u>1805.84*</u> , <u>1842.97*</u> , 1862.85*, 1881.73*, 1900.91, 1933.89, 1987.90, 2030.84*, 2079.90*, <u>2176.95*</u> , 2488.24*, 2536.23, 2637.11, 2664.32, 2809.18, 3137.45, 3162.28, 3209.44, 3271.40, 3289.37, 3339.44
P50/spot U3	<u>1130.47*</u> , 1144.50, 1196.05, <u>1313.67*</u> , <u>1326.04</u> , 1363.70*, 1379.70*, 1493.70*, 1742.05, 1765.74*, 1804.85*, <u>1805.82*</u> , 1843.92, 2810.17*
P29/spot U4	<u>1130.48*</u> , 1235.17, 1268.55, <u>1313.69*</u> , <u>1363.71*</u> , 1638.88*, <u>1647.73*</u> , 1804.87*, <u>1805.86*</u> , 1829.81, 1838.96, 1842.93*, 1862.87*, 2116.93, 2399.00, 2810.18*
P29/spot U5	1197.22, 1269.66, <u>1313.69*</u> , 1329.66, 1345.63*, 1351.61*, 1363.68*, 1375.57, 1379.68*, 1550.63*, 1638.84*, <u>1647.69*</u> , 1661, 71, 1704.74*, 1708.80, 1748.75*, 1761.81*, 1765.73*, 1804.80*, <u>1805.83*</u> , <u>1819.84</u> , <u>1842.91*</u> , 1862.83*, 1867.74, 1881.73*, 2079.85*, 2176.93*, 2383.95*, 2488.23*, 2501.21, 2504.23, 2705.13
P95	<u>1025.59</u> , 1100.57, 1114.57, 1179.61, 1242.66, 1300.54, 1326.65, 1328.64, 1344.68, 1357.64, 1386.67, 1405.68, <u>1457.72</u> , 1475.77, 1493.72*, 1657.75, 1670.79, <u>1687.83</u> , 1709.79, 1732.77, 1765.71*, 2028.58, <u>2069.98</u> , 2085.99, 2192.14, 2271.13, 2293.09, 2309.06, 2383.92*, <u>2399.22</u> , <u>2421.17</u> , 2828.03, 3312.25

*) Peptides of the same m/z common in different purified proteins. In bold: peptides that gave internal full or partial sequence by analysis of MS/MS spectra. Underlined: peptide analysed in MS/MS mode.

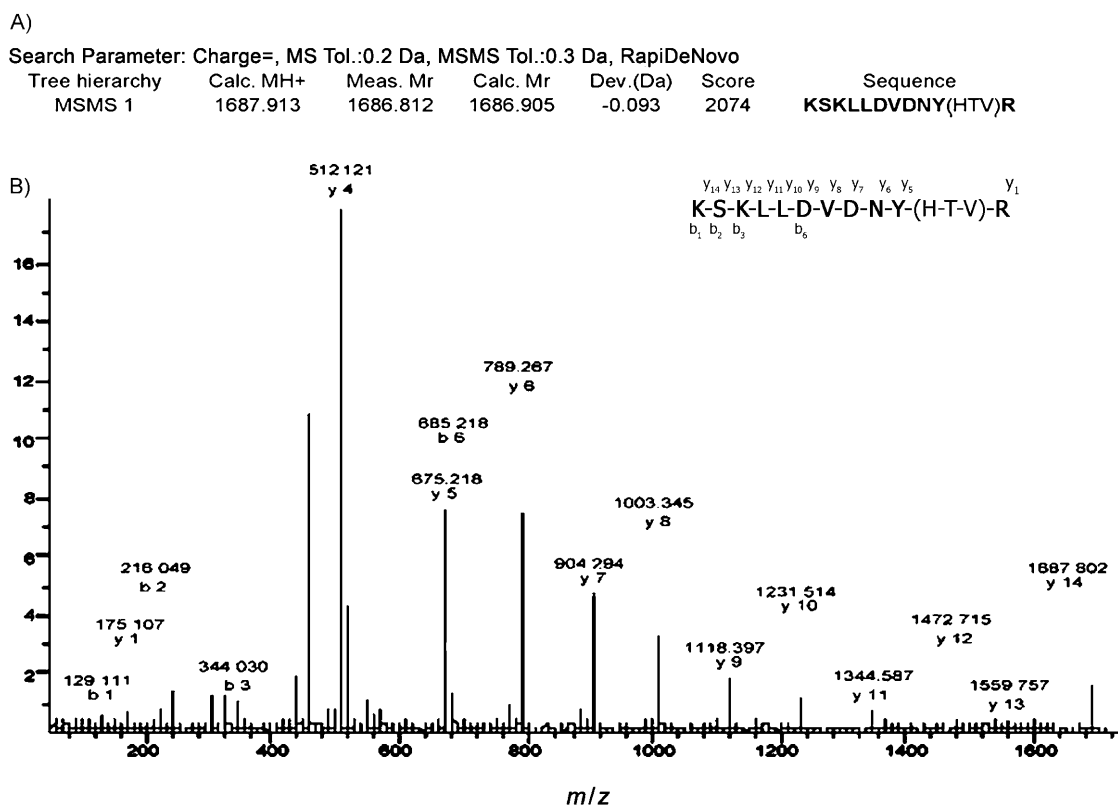


Figure 6. Example of de novo sequencing of a peptide obtained by trypsin digestion of purified matrix protein from *U. pictorum*. A) RapiDeNovo data with m/z 1687.83 from P95 trypsin hydrolysis. B) MS/MS spectrum acquired on MALDI-TOF/TOF. The de novo sequencing was performed by considering precise mass differences between adjacent b and y ions. In this example, the determination of the last four amino acids (-HTVR, in y4–y1 positions) was uncertain. Consequently, only the unambiguous sequence was considered further. The protein sequence data reported in the paper will appear in the UniProt knowledgebase under the accession numbers P85508–P85510.

Table 2. Full or partial (dash) de novo peptide sequences obtained after the tryptic digestion of purified ASM proteins of *Unio pictorum*. Sequences are deduced from MS/MS spectra.

Protein name (spot)	m/z	Charge	Mass [M+H] ⁺	Partial or full sequence	Accession no.
P95	1457.7	1 ⁺	1458.7	-TSHGGGKAG-	P85508
	1687.8	1 ⁺	1688.8	KSKLLDVNY-	
P50 (U2)	1313.7	1 ⁺	1314.7	KDALEHTGFAPK	P85509
	1647.7	1 ⁺	1648.7	KDGEEHVWVNY-	
P29 (U5)	1313.7	1 ⁺	1314.7	KDALEHTGFAPK	P85510

the biominerals. Nacre, widespread in shell-bearing molluscs, is one of the best studied shell structures. Furthermore, it is considered an ancestral shell texture,^[33] constituting a fascinating model for understanding the long-term evolution of molluscan mineralised tissues. In this paper we have characterised the matrix extracted from the nacreous layer of the freshwater bivalve *U. pictorum*. We detected a carbonic anhydrase enzymatic activity of the ASM and have described a novel, nacreous layer-specific, acidic glycoprotein, P95. In addition, we have used a proteomic approach for obtaining partial sequences, in order to compare the nacre proteins of this paleoheterodont bivalve with those previously published from pteriomorpha.

Carbonic anhydrase (CA) is a ubiquitous metalloenzyme, observed in animals, plants and bacteria, that reversibly catalyses the hydration of carbon dioxide, according to the equation $\text{CO}_2 + \text{H}_2\text{O} \rightleftharpoons \text{HCO}_3^- + \text{H}^+$. When intracellular or associated with the cytoplasm membranes, it displays an essential function for cytoplasmic acid/base balance and for transport mechanisms of CO_2 and carbonate ions.^[34] In addition, CA is essential in calcification processes,^[35] since it has been identified in several calcifying epithelia.^[36–38] One peculiarity of biomineralisation is the occurrence of CA activity in the extracellular skeletal matrix. This has been reported in only a few biological metazoan models: the cnidarian exoskeleton,^[39–40] crustacean calcium storage concretions,^[41] the fish otolith^[42] and the molluscan shell.^[9,42] The role of CA in an extracellular calcifying matrix is far from being elucidated. According to the mainstream hypothesis, CA catalyses the production of bicarbonate ions, which subsequently react with calcium to precipitate calcium carbonate. Alternately, it is also possible that in extracellular matrices, CA works in a different way, by catalysing the production of protons, which subsequently induce the dissolution of calcium carbonate.^[43] It is also possible that the CA activity is integrated in a multi-domain protein, such as nacrein, a shell protein that exhibits both CA activity and structural function,^[9] suggesting two successive spatio-temporal functions. Clearly, supplementary characterisations are needed before we can

draw conclusions on the significance of CA activity in the matrices associated to molluscan shells.

Among the proteins extracted from the shell of *U. pictorum*, P95 is a major component, specific to the nacre ASM. It is absent from the prismatic layer, unlike the other discrete components. This suggests that P95 might play an important function in controlling, inter alia, the building of nacre during shell formation. P95 is a glycoprotein, the acidity of which is entirely conveyed by its glycosyl moieties, consisting of acidic and sulfated polysaccharides. In its amino acid composition, P95 presents the "signature" of an acidic protein, because of its high Asx and Glx residue content.^[44] However, its deglycosylated protein core exhibits an experimentally determined pI of about 6.5–7, which classifies it as, at most, a moderately acidic protein. Such a value may appear surprising but is consistent with the distribution of the theoretical pI values (deduced from primary structures) of most of the molluscan shell proteins associated with nacre, which as a general rule are far less acidic than those extracted from calcitic shell layers.^[11] Another remarkable feature of P95 is its ability to bind calcium ions. Here again, this property is fully conveyed by the post-translational modifications of P95, in particular by the negatively charged sulfated sugars, and not by acidic amino acids. The presence of sulfated sugars in CaCO₃ biomineralisation products has been known for a long time,^[45] but their role is still unclear. In mollusc nacre, two putative functions have been proposed for them: concentration of calcium ions in the vicinity of the nucleating site by an ionotropic effect^[46–47] and mineral nucleation.^[48] Recent in situ experiments directed towards localizing sulfate groups at the surfaces of nacre tablets^[49] suggest that their function may be more diversified than expected, because they are not localised similarly in sheet (bivalvian) and columnar (cephalopod) nacles. Differential immunostaining of P95 and of deg-P95 directly on nacre, with more specific antibodies, may bring a more definitive answer.

In a given shell, what is the degree of similarity of the different proteins of the shell matrix? This question has only been touched upon, due to the fact that most of the published works characterise molluscan shell proteins individually. Recent studies have identified some "families", such as the nacrein, N14/16, asprich, shematin, or KRMP.^[11] So far, most of these families have been retrieved at the transcriptional level, and it is not clear yet whether all the members of a family are present together, because they have not been identified directly in the shell matrix. Our proteomic analysis of trypsin-digested 2DE spots and purified P95 shows that several peptides share the same *m/z* value. The MS/MS analysis of several of these peptides unambiguously demonstrates that some of them are identical. In one case, the similarity of these peptides is fully confirmed by the interpretation of fragmentation spectra for de novo sequencing. Our data demonstrate that short protein motifs can be used as "functional blocks" by different shell matrix proteins of clearly identified molecular mass. In a previous paper,^[50] we evoked this eventuality. These data tend to validate this hypothesis. Besides the possibility of cross-reactivity due to shared saccharidic epitopes, our proteomic data may also explain why strong cross-reactivity is recorded be-

tween an antibody raised against a single protein and other matrix components. These combined data have evolutionary implications and suggest that molluscan shell proteins were assembled, like "Meccano", by the tandem positioning of short functional modules, some of which are almost identical from one protein to another one. The genetic mechanism that underlies the process is unknown, but might be related to exon-shuffling.^[51] As we have pointed out, the alternative hypothesis involves a preferential cleavage of matrix proteins of high molecular weight into smaller fragments of determined mass during shell maturation, in a manner similar to that observed for tooth matrix proteins.^[52] Clearly, these two scenarios require further testing.

Experimental Section

Shell preparation and matrix extraction: Living *Unio pictorum* of 70–100 mm in length were collected in the Canal de Bourgogne (Dijon, France). For direct microscopic observation, cleaned, freshly fragmented shells were carbon-sputtered and observed in the secondary electron mode with a JEOL 6400 scanning electron microscope. The shell acid-soluble matrices (ASMs) of prismatic and nacreous layers were prepared as described previously.^[27]

One-dimensional SDS-PAGE: The separation of matrix components was performed under denaturing conditions by 1D SDS-PAGE in polyacrylamide gels (MiniProtean 3, 12%, Bio-Rad) as described by Laemmli.^[53] ASM (50 µg) was loaded into each well. Gels were stained with silver nitrate^[54] or with Coomassie Blue (Bio-Safe Coomassie, Bio-Rad). A protocol developed for staining unusually acidic proteins^[55] was also tested but produced blurred bands, and was not used further. To check the reproducibility of our extraction procedure, we performed several decalcifications from single shells, or from different batches of shells.

Carbonic anhydrase activity: The colorimetric method developed by Maren^[28] was performed to measure the carbonic anhydrase (CA) activity of the nacre ASM. The experiment was carried out under a stabilised flow of CO₂ in an ice-containing vessel. Phenol red (400 µL, 12.5 mg L⁻¹ in 2.6 mM NaHCO₃) was mixed with water (200 µL) and sample (100 µL). The reaction was initiated by addition of freshly made carbonate buffer (0.6 M Na₂CO₃, 0.412 M NaHCO₃, 100 µL), and the time interval until the colour change from red to yellow was monitored. This colour change characterises the pH drop of the solution (from 8.2 to 7.3) resulting from the production of protons during the reaction catalysed by the CA (CO₂ + H₂O → HCO₃⁻ + H⁺). The enzyme unit (EU) activity was calculated according to the following equation: activity units (EU) = (T₀ - T)/T, where T and T₀ are the reaction times required for the pH change with and without a catalyst, respectively. Acetazolamide was used as a specific inhibitor of the reaction. Heat inactivation of CA was performed by boiling the samples at 100 °C for 10 min.

Purification of proteins by preparative SDS-PAGE: The nacre ASM was fractionated on a preparative SDS polyacrylamide gel (8%) under denaturing conditions as described by Marin et al.^[56] Eighty fractions (5 mL each) were eluted from the preparative gel. Aliquots (100 µL) of each of them were tested by the dot-blotting technique (Bio-Dot apparatus, Bio-Rad) on PVDF membranes. The membranes were subsequently incubated with an antibody raised against the acid-soluble matrix of *Pinna nobilis* nacre. In previous experiments we had found that this polyclonal antibody cross-reacts with several molluscan matrices,^[57] including paleohetero-

don't bivalves such as *Unio* and *Anodonta* sp. Fractions of the same proteins were pooled, thoroughly dialysed for several days against MilliQ water at 4 °C and freeze-dried. The purity of the fractions was assessed on a mini-SDS-PAGE stained with silver nitrate.

Polyclonal antibodies against P95 and Western blot: Polyclonal antibodies raised against P95 were obtained by subcutaneous immunisation (100 µg P95 per injection) of a female New Zealand white rabbit by a standard procedure (Covalab, Lyon, France), at days 1, 14 and 28. The blood was collected at days 1 (preserum, 4–5 mL), 39 (first bleeding, 12–15 mL) and 56 (final bleeding, 4–5 mL). The serum containing the antibodies was used for Western blots. Briefly, the ASM and the purified P95 were run on SDS-PAGE, then blotted (120 mA, 90 min, Mini Trans Blot module, Bio-Rad) on a PVDF membrane. The membrane was treated as previously described,^[56] with a solution containing anti-P95 serum diluted 5000 times as the primary antibody.

For the animal experiments performed by the Covalab society, permission was obtained from the District Direction of the Veterinary Services (Burgundy, France; accreditation number A21231006).

Amino acid composition of P95: The amino acid composition of the purified fraction of P95 was determined by Eurosequence, Co. (Groningen, the Netherlands). After hydrolysis with HCl (5.7 N, 1.5 h at 150 °C), the resulting amino acids were analysed on an HP 1090 Aminoquant instrument by an automated two-step precolumn derivatisation with *o*-phthalaldehyde for primary and *N*-(9-fluorenyl)-methoxycarbonyl for secondary amino acids. Cysteine residues were quantified after oxidation.

Deglycosylation of P95: Chemical deglycosylation of P95 (1 mg) was performed in TFMS/anisole (2:1, v/v, 1.5 mL) at 0 °C for 3 h under N₂, with constant stirring as described by Edge et al.^[58] After neutralisation with cold pyridine (50%, 2 mL), the aqueous phase was extracted twice with diethyl ether and extensively dialysed against water (5 days) before being lyophilised. Fetuin was used as a positive control.

Polysaccharide staining and calcium-binding ability on gels: The glycosylation of P95 was studied qualitatively on denaturing minigels and on blots. In particular, saccharide moieties were investigated on minigels by use of Alcian Blue 8GX^[59] at pH 1 in order specifically to stain sulfated sugars,^[60] and by staining with PAS, which stains most carbohydrate residues.^[61] The calcium-binding ability of P95 and deglycosylated-P95 (*deg*-P95) was tested by two procedures: "Stains-All" staining on mini gels^[62] and ⁴⁵Ca overlay test on blots.^[63]

Growth of calcite crystals in the presence of ASM and purified P95: CaCO₃ precipitation was performed in vitro by slow diffusion of ammonium carbonate vapour in a calcium chloride solution.^[64] The test was adapted as follows: CaCl₂ (7.5 mM, 500 µL) containing different amounts of nacre ASM or purified P95 (0.1 µg mL⁻¹ to 20 µg mL⁻¹) was introduced onto eight-well culture slides (BD Falcon). Blank controls were performed without any sample. The culture slides were incubated 48 h at 4 °C in a closed desiccator containing crystals of ammonium bicarbonate. They were gently dried, carbon-sputtered and observed at 15 keV by scanning electron microscopy (JEOL 6400).

Separation of ASM proteins by 2DE: The nacre ASM was fractionated by 2DE. IEF was carried out with a Protean IEF cell (Bio-Rad). Precast 7 cm linear pH 3–10 immobilised pH gradient (IPG) strips were rehydrated, overnight, at 50 V (25 °C) with buffer (150 µL) containing ASM (80 µg) in urea (6 M), thiourea (2 M), 3-[(3-cholamidopropyl)dimethylammonio]-1-propanesulfonate (CHAPS; 4%,

w/v), dithiothreitol (DTT; 20 mM), ampholytes (0.1%) and bromophenol blue (0.001%). Immediately afterwards, focalisation was performed at 250 V for 15 min. The voltage was then set at 8000 V until it reached 10000 Vh. The IPG strips were subsequently incubated for 10 min in 2 mL equilibration buffer (6 M urea, 2% SDS, 375 mM Tris/HCl pH 8.8, 20% glycerol, 2 mL) containing DTT (130 mM), and then incubated for a further 10 min in the same buffer containing iodoacetamide (135 mM). Strips were rinsed in TGS (25 mM Tris, 192 mM glycine and 0.1% SDS), placed on top of precast NuPAGE® BisTris Novex SDS-PAGE (4–10%) and fixed with an overlay layer of agarose/TGS (0.5%, w/v). Electrophoresis was performed at 200 V for 40 min.

Protein digestion and MALDI-TOF/TOF analysis: After electrophoresis, gels were stained with Coomassie Blue before spot excision. Excised spots were washed for 10 min in NH₄HCO₃ (100 mM), and the supernatant was discarded. After incubation in ACN (100%, 20 µL) for 10 min, with gentle stirring, the supernatant was discarded, and samples were subsequently reduced with DTT (20 mM, 30 min, 56 °C in 0.1 M NH₄HCO₃) and alkylated with iodoacetamide (0.1 M, 20 min, 25 °C in 0.1 M NH₄HCO₃). Proteins were digested in gel with trypsin (10 µg mL⁻¹, 20 µL, ROCHE, France) in TFA (0.01%, 30 min at 4 °C), after which supernatant (17 µL) was discarded and pieces of gels were covered with NH₄HCO₃ solution (25 mM, 7 µL) for incubation (2 h, 37 °C). Peptide-containing liquid fractions were extracted by addition of TFA (0.5%, 1 µL), and the supernatant (around 11 µL) was recovered. The gel spots were rinsed with ACN (8 µL), and the supernatants were pooled. Digests were analysed with the MS and the MS/MS mode on a MALDI-TOF/TOF Ultraflex II instrument (Bruker Daltonics) with an α -cyano-4-hydroxycinnamic acid (HCCA) matrix. Purified P95 protein was similarly analysed on MS and MS/MS after trypsin digestion.

Mass spectrometry data and database searching: The mass spectra data were searched against the NCBI non-redundant database (October 2007), with the MASCOT search engine (<http://www.matrixscience.com>). The mass tolerance was 50 ppm for MALDI-TOF MS and 0.2 Da for MS/MS experiment with one missed cleavage. Other search parameters were carbamidomethyl as fixed modification and oxidation of methionine as variable modification. As no identification was achieved by MASCOT searching, MS/MS spectra were analysed and interpreted de novo manually with the assistance of the Rapid de Novo software. All the candidate sequences were merged into a MS BLAST search and were compared and aligned one by one with the other sequences of mollusc shell proteins, by use of the SIM tool from the ExPASy server (<http://www.expasy.ch/tools/sim.html>).

Acknowledgements

This work is supported by an ANR project for the period 2007–2010 (ACCRO-Earth, ref. BLAN06-2_159971, coordinator Gilles Ramstein, LSCE, Gif/Yvette). B.M. is financed by a PhD Fellowship (No. 15351), associated to an ACI from the Ministère Délégué à la Recherche et aux Nouvelles Technologies (JC3049, 2003–2006). The "Conseil Régional de Bourgogne" (Dijon, France) provided additional support for the acquisition of new equipment in the Biogeosciences research unit (UMR CNRS 5561). B.M. and F.M. thank Claudie Josse (Laboratoire de Réactivités des solides, University of Burgundy) for helping to handle the SEM, and Patrick Ducoroy, Géraldine Lucchi and Jean-Pascal Gimeno (IFR 100, Faculté de Médecine, Dijon) for their contribution to the MS/MS analysis.

Keywords: biomineralization · carbonic anhydrase · mollusc shell nacre · organic matrixes · two-dimensional electrophoresis

- [1] G. Goffinet, C. Jeuniaux, *Cah. Biol. Mar.* **1979**, *20*, 341–349.
- [2] S. Weiner, W. Traub, S. B. Parker, *Philos. Trans. R. Soc., B* **1984**, *304*, 425–434.
- [3] H. Nakahara in *Mechanisms and Phylogeny of Mineralization in Biological Systems* (Eds.: S. Suga, H. Nakahara), Springer, New York, **1991**, pp. 343–350.
- [4] K. Simkiss, K. M. Wilbur, *Biomaterialization: Cell Biology and Mineral Deposition*, Academic Press, San Diego, **1989**, pp. 1–337.
- [5] L. Addadi, D. Joester, F. Nudelman, S. Weiner, *Chem. Eur. J.* **2006**, *12*, 980–987.
- [6] S. Mann, *Nature* **1988**, *332*, 119–124.
- [7] G. Falini, S. Albeck, S. Weiner, L. Addadi, *Science* **1996**, *271*, 67–69.
- [8] D. Sud, D. Doumenc, E. Lopez, C. Milet, *Tissue Cell* **2001**, *33*, 154–160.
- [9] H. Miyamoto, T. Miyashita, M. Okushima, S. Nakano, T. Morita, A. Matsushiro, *Proc. Natl. Acad. Sci. USA* **1996**, *93*, 9657–9660.
- [10] C. Zhang, R. Zhang, *Mar. Biotechnol.* **2006**, *8*, 1–15.
- [11] F. Marin, G. Luquet, B. Marie, D. Medakovic, *Curr. Top. Dev. Biol.* **2007**, *80*, 209–276.
- [12] M. Kono, N. Hayashi, T. Samata, *Biochem. Biophys. Res. Commun.* **2000**, *269*, 213–218.
- [13] K. Mann, I. Weiss, S. André, H. Gabius, M. Fritz, *Eur. J. Biochem.* **2000**, *267*, 5257–5264.
- [14] I. M. Weiss, S. Kaufmann, K. Mann, M. Fritz, *Biochem. Biophys. Res. Commun.* **2000**, *267*, 17–21.
- [15] F. Marin, B. Corstjens, E. Gaulejac, E. De Vring-de Jong, P. Westbroek, *J. Biol. Chem.* **2000**, *275*, 20667–20675.
- [16] S. Sudo, T. Fujikawa, T. Nagakura, T. Ohkubo, K. Sakaguchi, M. Tanaka, K. Nakashima, T. Takahashi, *Nature* **1997**, *387*, 563–564.
- [17] M. Michenfelder, G. Fu, C. Lawrence, J. Weaver, B. Wustman, L. Taranto, J. Evans, D. E. Morse, *Biopolymers* **2003**, *70*, 522–533; erratum in M. Michenfelder, G. Fu, C. Lawrence, J. Weaver, B. Wustman, L. Taranto, J. Evans, D. E. Morse, *Biopolymers* **2004**, *73*, 291.
- [18] L. Treccani, K. Mann, F. Heinemann, M. Fritz, *Biophys. J.* **2006**, *91*, 2601–2608.
- [19] X. Shen, A. Belcher, P. Hansma, G. Stucky, D. E. Morse, *J. Biol. Chem.* **1997**, *272*, 32472–32481.
- [20] D. Jackson, C. McDougall, K. Green, F. Simpson, G. Wörheide, B. Degnan, *BMC Biol.* **2006**, *4*, 40–49.
- [21] D. Jackson, G. Wörheide, B. M. Degnan, *BMC Evol. Biol.* **2007**, *7*, 160–177.
- [22] L. Bédouet, F. Rusconi, M. Rousseau, D. Duplat, A. Marie, L. Dubost, K. Le Ny, S. Berland, J. Péduzzi, E. Lopez, *Comp. Biochem. Physiol. Part B* **2006**, *144*, 532–543.
- [23] L. Bédouet, A. Marie, L. Dubost, J. Péduzzi, D. Duplat, S. Berland, M. Puisségur, H. Boulzaguet, M. Rousseau, C. Milet, E. Lopez, *Mar. Biotechnol.* **2007**, *9*, 638–649.
- [24] J. G. Carter, *Skeletal Biomineralization: Patterns, Processes, and Evolutionary Trends*, Van Nostrand Reinhold, New York, **1990**.
- [25] J. Taylor, W. Kennedy, A. Hall, *Bull. Br. Mus. (Nat. Hist.) Zool. Lond.* **1969**, *3*, 1–125.
- [26] J. Taylor, *Palaeontology* **1973**, *16*, 519–534.
- [27] B. Marie, G. Luquet, J. P. Pais de Barros, N. Guichard, S. Morel, G. Alcaraz, L. Bollache, F. Marin, *FEBS J.* **2007**, *274*, 2933–2945.
- [28] T. Maren, *J. Pharmacol. Exp. Ther.* **1960**, *130*, 26–29.
- [29] S. Albeck, S. Weiner, L. Addadi, *Chem. Eur. J.* **1996**, *2*, 278–284.
- [30] Q. I. Feng, G. Pu, Y. Pei, F. Z. Cui, H. D. Li, T. N. Kim, *J. Cryst. Growth* **2000**, *216*, 459–465.
- [31] G. Fu, S. R. Qiu, C. A. Orme, D. E. Morse, J. J. De Yoreo, *Adv. Mater.* **2005**, *17*, 2678–2683.
- [32] A. Matsushiro, T. Miyashita, H. Miyamoto, K. Morimoto, B. Tonomura, A. Tanaka, K. Sato, *Mar. Biotechnol.* **2003**, *5*, 37–44.
- [33] J. Carter, G. R. Clark II in *Mollusk, Notes for a Short Course, Studies in Geology 13* (Ed.: T. W. Broadhead), University of Tennessee Press, Knoxville, **1985**, pp. 50–71.
- [34] S. Lindskog, *Pharmacol. Ther.* **1997**, *74*, 1–20.
- [35] K. M. Wilbur, L. H. Jodrey, *Biol. Bull. (Woods Hole, MA, USA)* **1955**, *108*, 359–365.
- [36] K. Mitsunaga, K. Akasaka, H. Shimada, Y. Fujino, I. Yasumasu, H. Numano, *Cell Differ.* **1986**, *18*, 257–262.
- [37] J. M. Lucas, L. W. Knapp, *Mar. Biol.* **1996**, *126*, 471–477.
- [38] Z. Yu, L. Xie, S. Lee, R. Zhang, *Comp. Biochem. Physiol. Part B* **2006**, *143*, 190–194.
- [39] M. A. Rahman, Y. Isa, T. Uehara, *Proteomics* **2005**, *5*, 885–893.
- [40] S. Tambutté, E. Tambutté, D. Zoccola, N. Caminiti, S. Lotto, A. Moya, D. Allemand, J. Adkins, *Mar. Biol.* **2007**, *151*, 71–83.
- [41] J. C. Meyran, F. Graf, J. Fournié, *Histochemistry* **1987**, *87*, 419–429.
- [42] G. Borelli, N. Mayer-Gostan, P. L. Merle, H. De Pontual, G. Boeuf, D. Allemand, P. Payan, *Calcif. Tissue Int.* **2003**, *72*, 717–725.
- [43] M. Chétail, J. Fournier, *Am. Zool.* **1969**, *9*, 983–990.
- [44] S. Weiner, *Calcif. Tissue Int.* **1979**, *29*, 163–167.
- [45] S. D. Douglas, H. D. Isenberg, L. S. Lavine, S. S. Spicer, *J. Histochem. Cytochem.* **1967**, *15*, 285–291.
- [46] E. M. Greenfield, D. C. Wilson, M. A. Crenshaw, *Am. Zool.* **1984**, *24*, 925–932.
- [47] L. Addadi, J. Moradian, E. Shay, N. G. Maroudas, S. Weiner, *Proc. Natl. Acad. Sci. USA* **1987**, *84*, 2732–2736.
- [48] M. Crenshaw, H. Ristedt in *The Mechanisms of Mineralization in the Invertebrates and Plants* (Eds.: N. Watabe, K. M. Wilbur), University of South Carolina Press, Columbia, **1976**, pp. 355–367.
- [49] F. Nudelman, B. Gotliv, L. Addadi, S. Weiner, *J. Struct. Biol.* **2006**, *153*, 176–187.
- [50] F. Marin, B. Pokroy, G. Luquet, P. Layrolle, K. De Groot, *Biomaterials* **2007**, *28*, 2368–2377.
- [51] L. Patthy, *Genetica* **2003**, *118*, 217–231.
- [52] J. P. Simmer, J. C. Hu, *Connect. Tissue Res.* **2002**, *43*, 441–449.
- [53] U. K. Laemmli, *Nature* **1970**, *227*, 680–685.
- [54] J. H. Morrissey, *Anal. Biochem.* **1981**, *117*, 307–310.
- [55] B. A. Gotliv, L. Addadi, S. Weiner, *ChemBioChem* **2003**, *4*, 522–529.
- [56] F. Marin, L. Peirera, P. Westbroek, *Protein Expression Purif.* **2001**, *23*, 175–179.
- [57] F. Marin, M. Gillibert, P. Westbroek, G. Muyzer, Y. Dauphin, *Geol. Mijnbouw* **1999**, *78*, 135–139.
- [58] A. S. Edge, C. R. Faltynek, L. Hof, L. E. Reichert, P. Weber, *Anal. Biochem.* **1981**, *118*, 131–137.
- [59] R. S. Wall, T. J. Gyi, *Anal. Biochem.* **1988**, *175*, 298–299.
- [60] R. Lev, S. Spicer, *J. Histochem. Cytochem.* **1964**, *12*, 309.
- [61] R. M. Zacharius, T. E. Zell, J. H. Morrison, J. J. Woodlock, *Anal. Biochem.* **1969**, *30*, 148–152.
- [62] K. P. Campbell, D. H. MacLennan, A. O. Jorgensen, *J. Biol. Chem.* **1983**, *258*, 11 267–11 273.
- [63] K. Maruyama, T. Mikawa, S. Ebashi, *J. Biochem.* **1984**, *95*, 511–519.
- [64] L. Addadi, S. Weiner, *Proc. Natl. Acad. Sci. USA* **1985**, *82*, 4110–4114.

Received: March 12, 2008

Published online on September 22, 2008